ZnO Nanoparticle Printing for UV Sensor Fabrication

van Ginkel, Hendrik Joost; Orvietani, Mattia ; Romijn, Joost; Zhang, Guo Qi Z; Vollebregt, Sten

DOI
10.1109/SENSORS52175.2022.9967053

Publication date
2022

Document Version
Final published version

Published in
Proceedings of the 2022 IEEE Sensors

ZnO NANOPARTICLE PRINTING FOR UV SENSOR FABRICATION

Hendrik Joost van Ginkel, Mattia Orvietani, Joost Romijn, Guo Qi Zhang, Sten Vollebregt

Electronic Components, Technology and Materials, Delft University of Technology, Delft, The Netherlands

h.j.vanginkel@tudelft.nl

***Abstract*— In this work, a novel microfabrication-compatible production process is demonstrated and used to fabricate UV photoresistors made from ZnO nanoparticles. It comprises a simple room-temperature production method for synthesizing and direct-writing nanoparticles. The method can be used on a wide range of surfaces and print a wide range of materials. Here, it is used to synthesize a ZnO photoresistor for the first time. The sensor shows a two orders of magnitude lower resistance under UV-C exposure compared to darkness. The low cost and simplicity of this synthesis method enables cheap integration of UV-C sensors for human exposure monitoring or UV-output monitoring of light sources.**

Keywords*— *UV sensor, nanoparticles, zinc oxide, spark ablation, printed electronics

I. INTRODUCTION

Wide band-gap semiconductors have attracted significant interest by the semiconductor industry [1]. They are typically hard materials that can operate at higher temperatures than conventional silicon technology and are largely insensitive to optical light [2,3,4]. This makes them excellent candidate materials for selective UV sensing, e.g. for flame detection or for monitoring the power output of UV appliances that are emerging in markets like disinfection, water treatment, etc [5]. One of the wide-bandgap semiconductors of interest for UV sensing is ZnO. ZnO has the benefit of having a direct 3.37 eV bandgap, is non-toxic, chemically and thermally highly stable, has a high radiation hardness, and is widely abundant [2,3,6,7,8]. These properties make ZnO an interesting material for UV sensors that are blind to visible light.

However, applying ZnO is not without difficulty. Zn has a high vapour pressure (6.8 Pa at 422 K) for a metal and will contaminate high vacuum systems [9]. For that reason, and for contamination concerns, its use is often restricted in most semiconductor processing equipment. Deposition is therefore done in dedicated equipment at low vacuum or atmospheric pressure and typically as the last process step. Common methods to deposit ZnO films are evaporating Zn or ZnO [8], sputtering [3,6,10], drop-casting suspended ZnO particles [11], or electroplating [12]. Although these methods can synthesize films of good quality, they require lithography for patterning. A back-end compatible process capable of local deposition on the sensing area would simplify sensor fabrication and reduce costs [8]. This would enable wider adoption for ZnO based devices and open up more possible application areas.

In this work, we propose a method that can direct-write ZnO nanoparticle deposits. The process reported here consists of a spark ablation generator and aerosol impaction printer, see fig. 1. The system only requires a carrier gas, metal electrodes and electricity. It has previously been used to write conducting metal tracks [13], for chemical sensor decoration, [14], and for catalysis [15]. The process can be used to synthesize and immediately deposit a wide range of metal(oxide) nanoparticles at room temperature and is compatible with a wide range of substrates, including flexible or rough substrates provided they are compatible with an ~1 mbar vacuum [16,17].

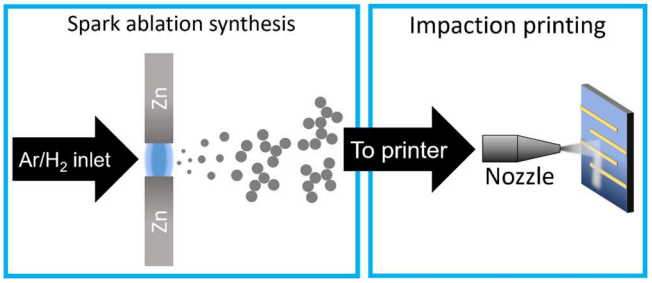

Figure 1. Schematic drawing of the process. Left: A repeating electrical spark (in blue) between two opposing Zn electrodes creates a vapour cloud which rapidly cools down to form nanoparticles (grey spheres) which eventually agglomerate. Right: The aerosol is led to an impaction printer where it is deposited on a device.

We demonstrate, for the first time, that ZnO nanoparticles deposited using spark ablation have a good UV detection capability when used as a photoresistor. Our first results demonstrate that the particles are fully oxidized zincite, show a two orders of magnitude decrease in resistivity when exposed to 265 nm UV, and determine the spectral response of the material.

II. METHODS

A. Substrate prepation

Si wafers were thermally oxidized to have a 300 nm SiO_2 insulating layer. Next, the electrodes were patterned using lithography and a 10/100 nm Cr/Au film was deposited. Lift-off with n-methylpyrrolidone (NMP) was performed to finish the electrode patterning process. The wafer was then diced in 10x10 mm dies and cleaned with acetone, isopropanol, and DI water. The final device has electrode spacings of 160 µm

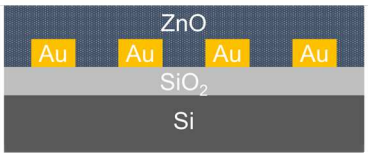

Figure 2. Schematic drawing of the photoresistor devices. Layers and components are not to scale.

2022 IEEE Sensors | 978-1-6654-8464-0/22/$31.00 ©2022 IEEE | DOI: 10.1109/SENSORS52175.2022.9967053

between each electrode. A cross-section of the device after coating with ZnO is shown in figure 2.

B. Nanoparticle synthesis and deposition

The nanoparticle synthesis was done with a VSP G1 (VSParticle B.V.) spark ablation generator operating at 3 mA and 1 kV. The spark ablation process is illustrated on the left side in figure 1. Spark ablation uses a repeating spark to ablate material from two opposing doped Zn electrodes (99.95% Zn, 0.05% Al). The resulting metal vapour is carried away by 1.5 l/min. Ar with 5% H_2 gas (1.0 bar) flowing around the electrodes. Ar/H_2 was used to suppress oxidation during deposition and allow the controlled oxidation of the sample after deposition [18]. This should improve particle-to-particle electrical contact. Due to high supersaturation caused by the rapidly cooling gas, nucleation occurs. The nuclei grow and when reaching a final size (5-20 nm, depending on settings), they start to agglomerate [16,17].

The resulting aerosol is then passed to an impaction printer where a pressure drop over a nozzle accelerates the gas. The inertia of the nanoparticles causes them to impact on the substrate surface with enough force to be immobilized. A programmable XYZ-orientable nozzle enables the tool to print complex patterns. The impaction printer is operated at 0.52 mbar with a 0.32 l/min nozzle placed at a 1 mm distance to the sample surface. The deposition process is shown on the right side of figure 1. After deposition, the samples were annealed at 600 °C for six hours in an N_2 atmosphere to complete the oxidation and improve conductivity through sintering.

C. Characterization

Structure characterization was done with scanning electron microscopy (SEM, Hitachi Regulus 8230) operated at 5 kV acceleration voltage and by x-ray diffraction (XRD, Brucker D8 diffractometer with Cu Kα radiation).

To measure the photoresponse of the ZnO devices, two setups were used. The first uses a Microtech probe station equipped with a 5 mW 265 nm LED to measure the charging and discharging time under UV-C exposure. A second, spectral responsivity setup was used to measure the generated current per wavelength. It consists of a combination of a deuterium and a halogen lamp (Bentham D2-QH Deuterium-Halogen Source), whose output is connected to a monochromator (Horiba iHR320). The selected wavelength is moved to the exit slit of the latter device and is then focused on the sample by a UV reflective mirror (CM750-200-F01). The relative output of the photodetector is expressed as voltage per wavelength and an optimal readout circuit has been designed to read out low output voltages.

III. RESULTS

A. Structure

After deposition and annealing, the sample shows cracking around the edges of the printed lines, as can be seen in figure 3A. This is likely due to restructuring during annealing and bad adhesion to the SiO_2 surface. In the middle of the line, where the deposit is the thickest, the cracks are much smaller. At higher magnification, as seen in figure 3B,

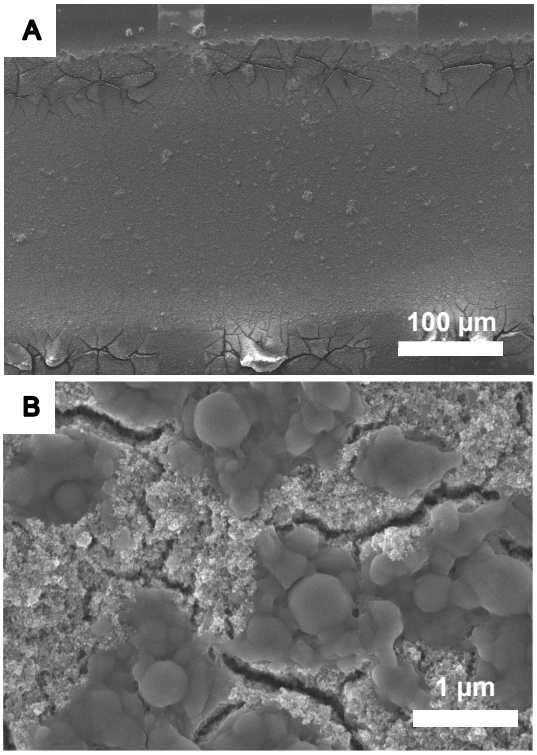

Figure 3. SEM images (Hitachi Regulus 8230, 5 kV) of a nanoparticle deposit on top of electrodes showing cracking at the edges. Note there is no such cracking above the Au electrodes. Inset: close-up in the middle of the line.

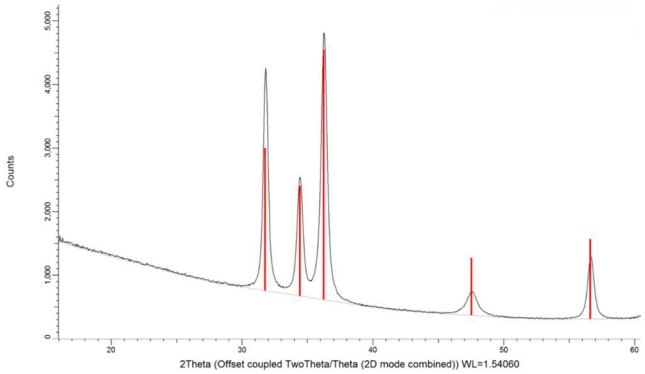

Figure 4. XRD results on a ZnO sample. Red bars indicate the diffraction pattern of zincite.

the nanoporous structure becomes visible and we can observe locally coalesced areas next to micro-cracks. These areas are also formed during the restructuring and possibly local melting of partially oxidized Zn. The thicker area of the film has too much structural strength for cracks to propagate as far as near the edges. Deposition of an adhesion layer would vastly improve the adhesion and reduce delamination and cracking. Removal of cracks would be possible by layered deposition with multiple deposition-annealing cycles to fill any emerging cracks.

The XRD result in figure 4 shows only a zincite phase and no pure Zn crystallites were seen, indicating the sample has been fully oxidized as intended. We also see high crystallinity due to the

B. *Conductivity and UV sensing*

Using a 265 nm LED, four-point-probe IV measurements were done. Despite the micro-cracks the structure electrically conducts. The results shown in figure 5 show Ohmic responses with film resistance of $5.02*10^{10}$ Ω when in complete darkness and $5.82*10^{8}$ Ω when exposed to 265 nm light. This is a nearly two orders of magnitude resistance reduction under UV illumination. As seen in figure 6, it takes several minutes to reach a stable current before and after illumination. The charging time to reach 90% of the plateau value is 79 seconds and discharging to 10% takes 82 seconds. Although the charging and discharge time is slower than other devices reported in literature, the two orders of magnitude response is comparable to other devices [2,3,6,8,10,11]. Considering these are first results of a new, flexible synthesis method with minimal optimization in the design and synthesis process, these values can be expected to improve.

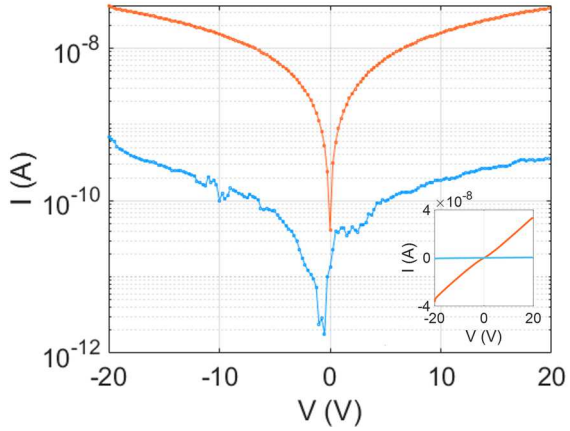

Figure 5. Semilogarithmic IV curves in darkness (blue) and under 265 nm illumination (orange). Inset: The same data plotted with linearly y-axis.

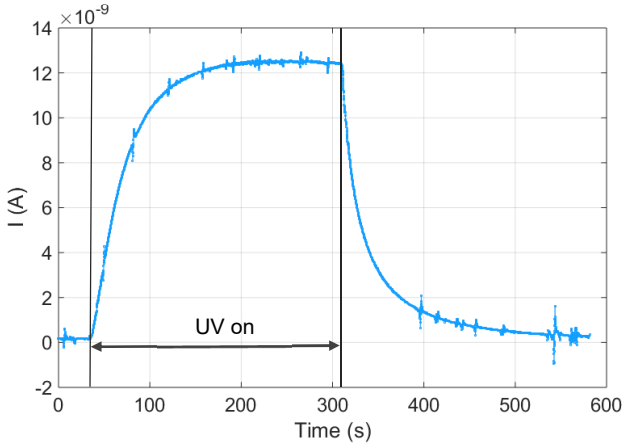

Figure 6. Photo-response curve showing charging and discharging when exposure to 265 nm light starts or stops. Measurement done at 5 V.

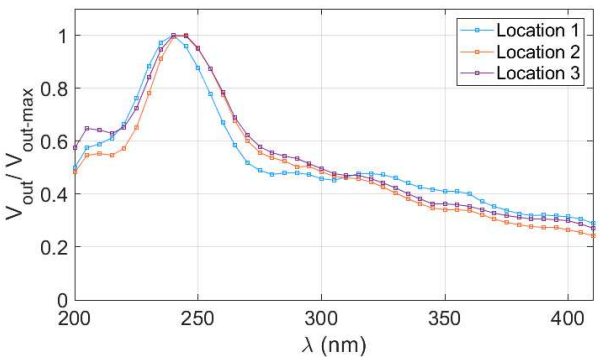

Figure 7. Response per wavelength between 200 and 410 nm for three measurements on one printed ZnO line at a 5 V bias. The curve is normalized for comparison, since changes in illumination intensity and film resistance at different locations affect the response.

The photogenerated current at different wavelengths was measured. Figure 7 shows the spectral response between 200 and 410 nm. Each point was acquired after a 5 min waiting time to ensure the current had stabilized. We can observe a maximum at 240 nm with a steep decline until 280 nm, after which the current slowly keeps declining. With a 3.37 eV bandgap, one would expect photocurrent drop for higher wavelengths than 368 nm. Having an irradiating optical spot bigger than the device itself hampers asserting the light intensity of the measurement. Slight changes in sample location between measurements will therefore change the measured voltage. Future work should add a calibrated reference sensor in parallel to the sample to measure the light intensity during each measurement.

IV. Conclusion

A method to print ZnO films on a broad range of substrates is presented with the first results of UV sensors fabricated this way. The resulting film has a nanoporous structure with partially coalesced areas and is conducting despite crack formation. Under UV-C illumination, resistance is reduced by two orders of magnitude compared to complete darkness, comparable with devices from literature. Charging and discharging times are long, but the devices are relatively large and not optimized yet. Future work should focus on optimization of the sensor design to improve response time and sensitivity. Furthermore, a study for better annealing recipes to reduce resistivity and increase responsivity is needed to further improve the material.

Acknowledgment

We would like to acknowledge the funding provided by NWO grant 729.001.023. We thank VSParticle B.V. for the use of their equipment. We also thank the Else Kooi Lab for facilitating the experiments.

REFERENCES

[1] P. R. Wilson et al., "IEEE ITRW: International Technology Roadmap for Wide-Bandgap Power Semiconductors: An Overview," IEEE Power Electronics Magazine, vol. 5, no. 2, Art. no. 2, Jun. 2018, doi: 10.1109/mpel.2018.2821938

[2] P. S. Shewale and Y. S. Yu, "UV photodetection properties of pulsed laser deposited Cu-doped ZnO thin film," Ceramics International, vol. 43, no. 5, Art. no. 5, Apr. 2017, doi: 10.1016/j.ceramint.2016.12.041.

[3] X. Liu et al., "All-printable band-edge modulated ZnO nanowire photodetectors with ultra-high detectivity," Nature Communications, vol. 5, no. 1, Art. no. 1, Jun. 2014, doi: 10.1038/ncomms5007.

[4] J. Romijn et al., "Visible Blind Quadrant Sun Position Sensor in a Silicon Carbide Technology," Jan. 2022, doi: 10.1109/mems51670.2022.9699533.

[5] G. Knight, "Monitoring of ultraviolet light sources for water disinfection," doi: 10.1109/ias.2004.1348537.

[6] H. S. Al-Salman and M. J. Abdullah, "Fabrication and Characterization of Undoped and Cobalt-doped ZnO Based UV Photodetector Prepared by RF-sputtering," Journal of Materials Science & Technology, vol. 29, no. 12, Art. no. 12, Dec. 2013, doi: 10.1016/j.jmst.2013.10.007.

[7] S. J. Pearton et al., "Recent advances in processing of ZnO," Journal of Vacuum Science & Technology B: Microelectronics and Nanometer Structures, vol. 22, no. 3, Art. no. 3, 2004, doi: 10.1116/1.1714985.

[8] S. K. Panda and C. Jacob, "Preparation of transparent ZnO thin films and their application in UV sensor devices," Solid-State Electronics, vol. 73, pp. 44–50, Jul. 2012, doi: 10.1016/j.sse.2012.03.004.

[9] J. D. McKinley and J. E. Vance, "The Vapor Pressure of Zinc between 150C and 350C," The Journal of Chemical Physics, vol. 22, no. 6, Art. no. 6, Jun. 1954, doi: 10.1063/1.1740276.

[10] Z. Ke et al., "Low temperature annealed ZnO film UV photodetector with fast photoresponse," Sensors and Actuators A: Physical, vol. 253, pp. 173–180, Jan. 2017, doi: 10.1016/j.sna.2016.07.026.

[11] A. J. Gimenez et al., "ZnO-Paper Based Photoconductive UV Sensor," The Journal of Physical Chemistry C, vol. 115, no. 1, Art. no. 1, Dec. 2010, doi: 10.1021/jp107812w.

[12] S. N. Sarangi, "Controllable growth of ZnO nanorods via electrodeposition technique: towards UV photo-detection," Journal of Physics D: Applied Physics, vol. 49, no. 35, Art. no. 35, Aug. 2016, doi: 10.1088/0022-3727/49/35/355103.

[13] H. J. van Ginkel et al., "High Step Coverage Interconnects By Printed Nanoparticles," in 2021 23rd European Microelectronics and Packaging Conference & Exhibition (EMPC), 2021, pp. 1–4, doi: 10.23919/empc53418.2021.9585005.

[14] H. Avdogmus et al., "Dual-Gate Fet-Based Charge Sensor Enhanced by In-Situ Electrode Decoration in a MEMS Organs-On-Chip Platform," Jun. 2021, doi: 10.1109/transducers50396.2021.9495393.

[15] R. Becker et al., "A Scalable High-Throughput Deposition and Screening Setup Relevant to Industrial Electrocatalysis," Catalysts, vol. 10, no. 10, Art. no. 10, Oct. 2020, doi: 10.3390/catal10101165.

[16] T. V. Pfeiffer et al., "New developments in spark production of nanoparticles," Advanced Powder Technology, vol. 25, no. 1, Art. no. 1, 2014, doi: 10.1016/j.apt.2013.12.005.

[17] A. Schmidt-Ott, Spark Ablation: Building Blocks for Nanotechnology, 1st ed. Jenny Stanford Publishing, 2020.

[18] R. T. Hallberg et al., "Hydrogen-assisted spark discharge generated metal nanoparticles to prevent oxide formation," Aerosol Science and Technology, vol. 52, no. 3, Art. no. 3, Dec. 2017, doi: 10.1080/02786826.2017.1411580.